

Theory versus experiment for a family of single-layer compounds with a similar atomic arrangement: (Tl, X)/Si(111) $\sqrt{3}\times\sqrt{3}$ ($X = \text{Pb, Sn, Bi, Sb, Te, Se}$)

A. V. Matetskiy,¹ I. A. Kibirev,^{1,2} A. N. Mihalyuk,^{1,2} S. V. Ereemeev,^{3,4} D. V. Gruznev,¹ L. V. Bondarenko,¹
A. Y. Tupchaya,¹ A. V. Zotov,^{1,2} and A. A. Saranin^{1,2}

¹*Institute of Automation and Control Processes FEB RAS, 690041 Vladivostok, Russia*

²*School of Natural Sciences, Far Eastern Federal University, 690091 Vladivostok, Russia*

³*Institute of Strength Physics and Materials Science, 634021 Tomsk, Russia*

⁴*Department of Physics, Tomsk State University, 634050 Tomsk, Russia*

(Received 28 April 2017; revised manuscript received 22 June 2017; published 7 August 2017)

Two-dimensional compounds made of one monolayer of Tl and one-third monolayer of Pb, Bi, Te, or Se (but not of Sn or Sb) on Si(111) have been found to have a similar atomic arrangement which can be visualized as a $\sqrt{3}\times\sqrt{3}$ -periodic honeycomb network of chained Tl trimers with atoms of the second adsorbate occupying the centers of the honeycomb units. Structural and electronic properties of the compounds have been examined in detail theoretically using density functional theory (DFT) calculations and experimentally using low-energy electron diffraction (LEED), scanning tunneling microscopy (STM), and angle-resolved photoelectron spectroscopy (ARPES) observations. It has been found that though structural parameters of the compounds are very similar for all species, the only common feature of their band structure is a considerable spin-splitting of the surface-state bands, while other basic electronic properties vary greatly with a change of species. The Tl-Pb compound is strongly metallic with two metallic surface-state bands; the Tl-Bi compound is also metallic but with a single metallic band; the Tl-Te and Tl-Se compounds appear to be insulators.

DOI: [10.1103/PhysRevB.96.085409](https://doi.org/10.1103/PhysRevB.96.085409)

I. INTRODUCTION

Metal/silicon surface reconstructions have attracted considerable attention from researchers due to abundance of their structural and electronic properties. One of the promising direction within this research field is associated with going beyond the case of a single adsorbate and studying phenomena occurring upon coadsorption of two or more species. Taking into account a large number of possible combinations of atomic species, the number of the potentially advanced systems could be quite large. In this respect, one-atom-layer compounds can be treated as a novel class of low-dimensional materials that awaits an exploration of their physical properties [1]. Some advanced properties of such compounds still remain hypothetical, e.g., theoretically predicted properties of a two-dimensional (2D) topological insulator for a number of compounds on Si(111) [2–6]. However, occurrence of some advanced properties has already been proved experimentally, including extremely high electron velocity at the Fermi level in (Sn, Ag)/Si(111) [1] and (Tl, Sn)/Si(111) [7], giant spin splitting of metallic surface-state bands in adsorbate-modified Au/Si(111) [8], (Bi, Na)/Si(111), and (Tl, Pb)/Si(111) [9], unusual spin texture in (Au, Al)/Si(111) [10], and superconductivity in (Tl, Pb)/Si(111) [11]. The last compound, (Tl, Pb)/Si(111), is of especial promise as it combines together 2D superconductivity with a giant Rashba effect [11]. This one-atom-layer compound is made of one monolayer (ML, $7.84 \times 10^{14} \text{ cm}^{-2}$) of Tl and one-third ML of Pb and has a $\sqrt{3}\times\sqrt{3}$ periodicity. Its atomic arrangement can be visualized as a honeycomb network of chained Tl trimers with Pb atoms occupying the centers of the honeycomb units.

In the present study, we explored the possibility of the formation of the surface compounds having a similar atomic arrangement except for the Pb atoms being replaced by Sn, Bi, Sb, Te, or Se. To check the stability of these

hypothetical compounds, density functional theory (DFT) calculations were employed. The calculation results are compared with the experimental data obtained with scanning tunneling microscopy (STM) and angle-resolved photoelectron spectroscopy (ARPES).

II. CALCULATION AND EXPERIMENTAL DETAILS

To study the Tl-X 2D systems on Si(111) we use simulations based on the density functional theory (DFT) as implemented in the Vienna *ab initio* simulation package (VASP) [12]. The wave functions and potentials are generated within the projector-augmented wave (PAW) method [13]. The local density approximation (LDA) has been used for the exchange correlation potential. Relativistic effects, including spin-orbit interaction (SOI), were taken into account.

To simulate the Si(111) substrate we use a slab consisting of 10 bilayers (BL) of silicon. Hydrogen atoms were used to passivate the Si dangling bonds at the bottom of the slab. Both the bulk Si lattice constant and the atomic positions of adsorbed atoms and atoms of Si layers within the three BLs of the slab were optimized, including SOI self-consistently. Silicon atoms of the deeper layers were kept fixed at the bulk crystalline positions. The geometry optimization is performed until the residual force was smaller than $5 \text{ meV}/\text{\AA}$.

For band structure calculations we apply an approximate quasiparticle approach, DFT-1/2 [14,15], which has previously shown excellent results for band gaps in semiconductors [14]. The characteristic r_{cut} parameter—that is, the cutoff radius applied for the self-energy potential included in the exchange-correlation functional, for the excited holes in Si p orbitals—is calculated for our optimized bulk silicon to be 1.919 \AA . The obtained direct and indirect band gaps of 2.90 and 1.09 eV, respectively, are very close to the experimental values (3.05

and 1.17, respectively [16]). Note that the obtained r_{cut} just a little bit differ from the value of 1.942 Å found in the original paper, Ref. [14], where experimental lattice parameters and ultrasoft pseudopotentials were used.

The main experiments were performed in the UHV Omicron MULTIPROBE system equipped with low-energy electron diffraction (LEED), STM, x-ray photoelectron spectroscopy (XPS) and ARPES facilities. Atomically-clean Si(111)7×7 surfaces were prepared *in situ* by flashing to 1280 °C after the samples were first outgassed at 600 °C for several hours. Thallium was deposited from a tantalum-tube effusion cell. Pristine Tl/Si(111)-1×1 reconstruction was prepared by depositing 1 ML Tl onto Si(111)-7×7 surface held at ~300 °C. Growth of the Tl-Pb, Tl-Sn, Tl-Sb, and Tl-Bi compounds were conducted in the same UHV system using Pb or Sn-stuffed Mo-tube effusion cells and Sb or Bi-filled BN crucibles, respectively. Growth of the Tl-Te and Tl-Se compounds was conducted in a separate MBE chamber equipped with reflection high-energy electron diffraction (RHEED) and organic-material-effusion cells (Dr. Eberl MBE-Komponenten GmbH) for deposition of Te and Se. The prepared (Tl, Te)/Si(111) and (Tl, Se)/Si(111) samples were transferred into the UHV Omicron MULTIPROBE system for analysis. Transportation was realized without breaking the UHV conditions using the evacuated transfer unit with a base pressure of better than 1.0×10^{-9} Torr. STM images were acquired in a constant-current mode with a mechanically cut PtIr tip after annealing in vacuum. ARPES measurements were conducted using VG Scienta R3000 electron analyzer and high-flux He discharge lamp with toroidal-grating monochromator as a light source for 21.2 eV photons.

III. RESULTS AND DISCUSSION

A. Calculation results

Figure 1(a) shows a basic structural model of the (Tl, X)/Si(111) $\sqrt{3} \times \sqrt{3}$ system which validity has recently been proved for Tl-Pb compound [9] and which is tested in the present work as a hypothetical structure for compounds with $X = \text{Sn, Bi, Sb, Te}$ and Se . As one can see, the basic structure is built of the chained Tl trimers arranged into a honeycomb network, while atoms of the second adsorbate, X , occupy the centers of the honeycomb units. The centers of Tl trimers as well as residence of X atoms are in the T_1 (on-top) sites.

DFT calculations reveal the principal stability of this basic structure for each X species from the above list. There is a certain variation of the structural parameters depending on the species. For example, Pb and Sn atoms reside higher than Tl atoms by ~0.4 and ~0.25 Å, respectively, Bi and Sb atoms are almost at the Tl level (height difference is less than 0.1 Å), while Te and Se are located lower than Tl by ~0.3 and ~0.4 Å, respectively [Fig. 1(b)]. The Tl trimer size (i.e., the Tl-Tl bond length in the trimer) is almost the same, slightly below ~3.31 Å for all species except for the case of Se where it amounts to ~3.33 Å [Fig. 1(c)]. The Tl trimer is almost aligned along the principal crystallographic direction of Si(111) for all species (the rotation angle varies in between 0.8° and 1.5°) again except for Se where the Tl trimer is twisted by 7.4° [Fig. 1(d)].

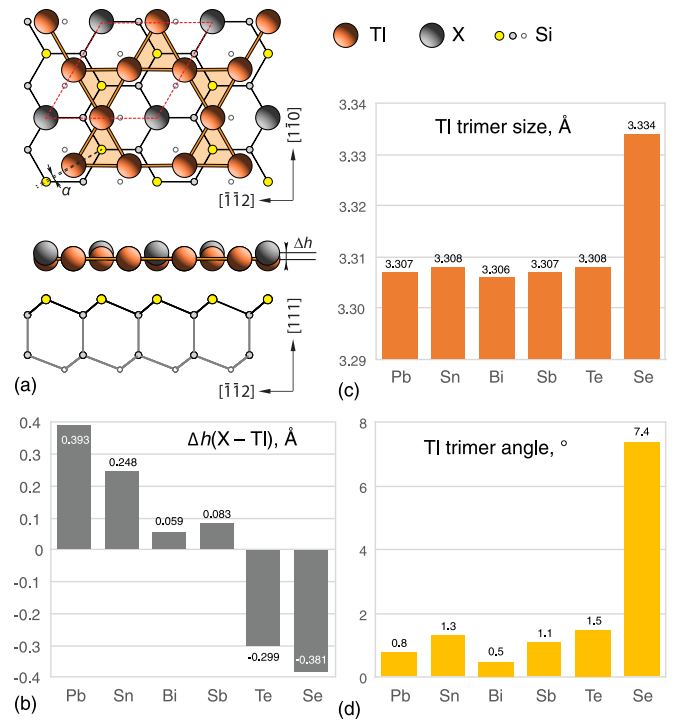


FIG. 1. (a) Structural model of the (Tl, X)/Si(111) $\sqrt{3} \times \sqrt{3}$ system and its structural characteristics, including (b) difference in heights of X and Tl atoms with respect to the top Si bilayer, Δh , (c) Tl trimer size (the Tl-Tl bond length in the trimer), and (d) Tl-trimer rotation angle with respect to the Si(111) $[1\bar{1}0]$ direction, for $X = \text{Pb, Sn, Bi, Sb, Te}$, and Se . In (a) Tl atoms are shown by red circles, X atoms by dark gray circles, Si atoms by yellow circles in T_1 sites, light grey circles in T_4 sites and small white circles in the second Si bilayer. The inner areas of Tl trimers are hatched with orange color for better visualization of the chained trimer network. The $\sqrt{3} \times \sqrt{3}$ unit cell is outlined by a dashed red frame.

Figure 2 shows calculated band structures of the (Tl, X)/Si(111) $\sqrt{3} \times \sqrt{3}$ systems. One can see that a Rashba spin-splitting of the surface-state bands is characteristic feature for all systems under consideration. The surface states of Tl and X species compounds mainly come from Tl- s , Tl- $p_{x,y,z}$, X - $p_{x,y}$ with negligible contribution from X - s and X - p_z orbitals. The main difference is in the metallicity which decreases when the X species change from those of Group IV (Pb and Sn) to Group V (Bi and Sb) and then to Group VI (Te and Se). This change in the band structure occurs mainly owing to the charge transfer from Tl atoms to Si, which is the result of appropriate charge transfer from Si to X species as shown in Fig. 3. The latter strongly increases from about -0.7 to 0.8 electrons for Group IV (Pb and Sn), to nearly zero for Group V (Bi and Sb) and then to about 1.3–1.5 for Group VI (Te and Se) as the result of the increase of the electronegativity. The Tl-Pb and Tl-Sn compounds demonstrate the greatest metallicity, having two dispersed spin-split bands crossing the Fermi level. The Tl-Bi and Tl-Sb compounds are also metallic but their dispersed bands are located lower as compared to those of Tl-Pb and Tl-Sn compounds; as a result only one metallic band remains. With changing X for Te and Se the bands go further down and

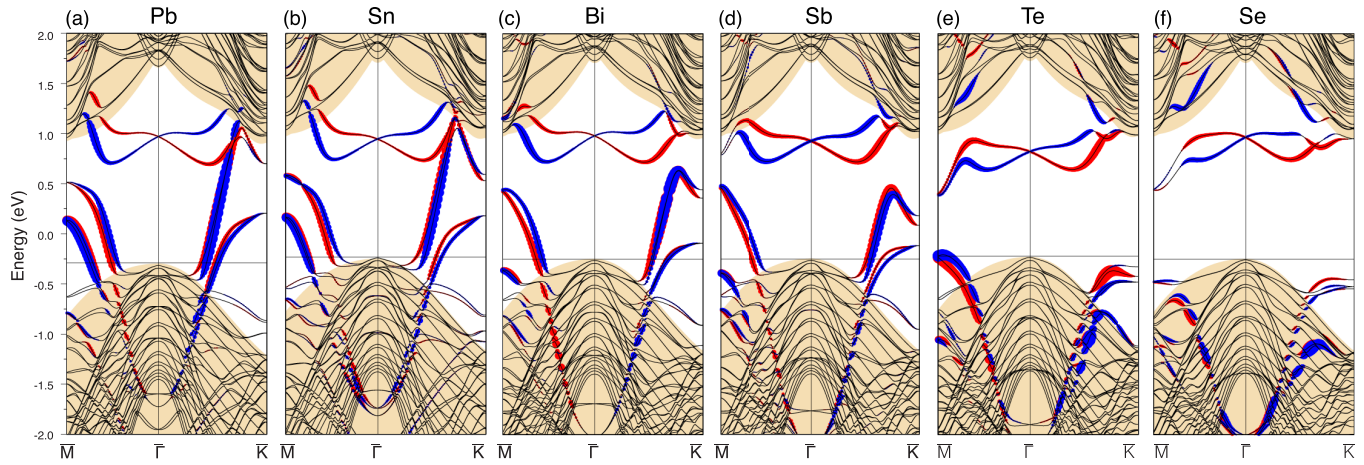


FIG. 2. Calculated electron band structures of the $(\text{Tl}, X)/\text{Si}(111)\sqrt{3}\times\sqrt{3}$ systems where $X =$ (a) Pb, (b) Sn, (c) Bi, (d) Sb, (e) Te, and (f) Se along the $\bar{M}-\bar{\Gamma}-\bar{K}$ directions within the $\sqrt{3}\times\sqrt{3}$ surface Brillouin zone. The bands with opposite spin orientations are highlighted by blue and red circles. The size of the circles corresponds to the strength of the surface character summed over all orbitals at a particular k_{\parallel} value. Shaded regions indicate projected bulk bands.

reside now well below the Fermi level, hence the Tl-Te and Tl-Se compounds show up as insulators.

B. Comparison with experiment

Let us consider now an accordance of the calculated data to the results of experimental observations. Recall that a nice correspondence has already been reported for $(\text{Tl}, \text{Pb})/\text{Si}(111)\sqrt{3}\times\sqrt{3}$, where simulated STM images and calculated band structure reproduce experimental STM and ARPES data in great detail [9] (see Fig. 4). Recall also that, to prepare a completed Tl-Pb compound layer, 1/3 ML of Pb was deposited onto the Tl/Si(111) 1×1 surface with 1.0 ML of Tl held at room temperature (RT), followed sometimes by a mild (e.g., ~ 150 °C) annealing to improve structural quality of the compound layer. A similar preparation procedure was used for other X species.

It is worth noting, however, that not all of the hypothetical Tl- X compounds having a structure as in Fig. 1(a) form in reality. For example, the Tl-Sn compound, though displaying a same $\sqrt{3}\times\sqrt{3}$ periodicity, has been proved to have another arrangement; namely, it shows up as atomic sandwich in which 1.0 ML of Sn resides on Si(111) substrate and 1.0 ML of Tl is located above the Sn layer [7] (see inset in Fig. 5). It forms from

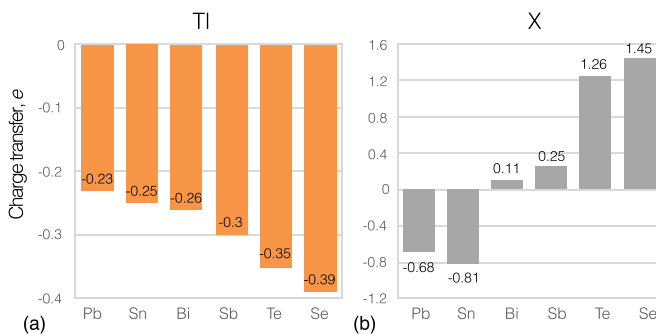


FIG. 3. Calculated electron charge transfer from (a) Tl atoms and (b) X atoms as a result of the 2D Tl- X compound formation on Si(111).

the early stages of Sn deposition, and after depositing 1/3 ML of Sn it just occupies about one-third of the surface area with the other area being still covered by a pristine 1×1 -Tl phase (Fig. 5). DFT calculations demonstrate that Tl-Sn compound having composition of 1.0 ML of Tl and 1.0 ML of Sn is energetically preferable over compound with 1.0 ML of Tl and 1/3 ML of Sn by 41 meV per 1×1 unit cell. That explains a preference for the formation of the Tl (1.0 ML)–Sn (1.0 ML) compound in the $(\text{Tl}, \text{Sn})/\text{Si}(111)$ system. For comparison, in the $(\text{Tl}, \text{Pb})/\text{Si}(111)$ system the compound with 1/3 ML of Pb has a formation energy by 105 meV per 1×1 unit cell lower than that of the compound with 1.0 ML of Pb, hence the Tl (1.0 ML)–Pb(1/3 ML) compound is observed in reality.

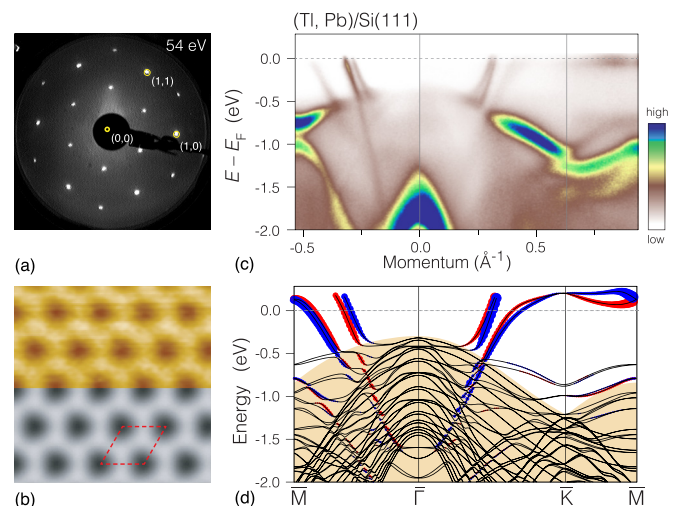


FIG. 4. (a) LEED pattern [with the main reflections, (0,0), (1,0) and (1,1) being highlighted by yellow circles to guide the eye]; (b) empty-state (+0.4 V) STM image (upper and lower halves correspond to experimental and simulated STM images, respectively); (c) experimentally determined and (d) calculated band dispersions for the $(\text{Tl}, \text{Pb})/\text{Si}(111)$ surface. The part of the ARPES spectrum recorded in the $\bar{\Gamma}-\bar{M}$ direction has been symmetrized with respect to the \bar{M} point.

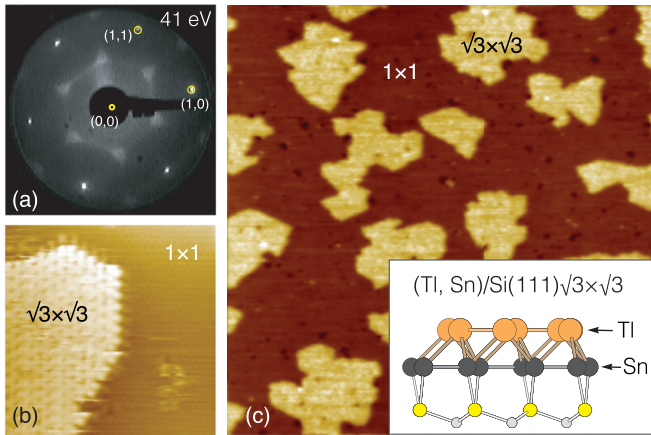


FIG. 5. (a) LEED pattern and (b) $120 \times 120 \text{ \AA}^2$ and (c) $1000 \times 1000 \text{ \AA}^2$ filled-state (-1.0 V) STM images from $\text{Ti}/\text{Si}(111)1 \times 1$ surface after deposition of $\sim 0.3 \text{ ML}$ of Sn onto it. The bright regions (which occupy about 30% of a surface area) correspond to the Ti-Sn compound. The dark area is occupied by pristine 1×1 -Ti reconstruction. The inset in (c) shows a side view of the Ti-Sn compound sandwich-like structure as determined in Ref. [7]. Ti atoms are shown by red circles, Sn atoms by dark gray circles, and Si atoms by yellow circles in T_1 sites and by light grey circles in T_4 sites.

Formation of Ti-Bi compounds on Si(111) has been reported to obey an unusual growth mode due its specific tiling structure built not by a translation of a single unit cell but by a quasiperiodic stacking of three different tiling elements [17]. Nevertheless, the Ti-Bi compound with $\sim 0.36 \text{ ML}$ of Bi can be thought as containing domains of the $\sqrt{3} \times \sqrt{3}$ -Ti, Bi structure as in Fig. 1(a) bounded by domain walls.

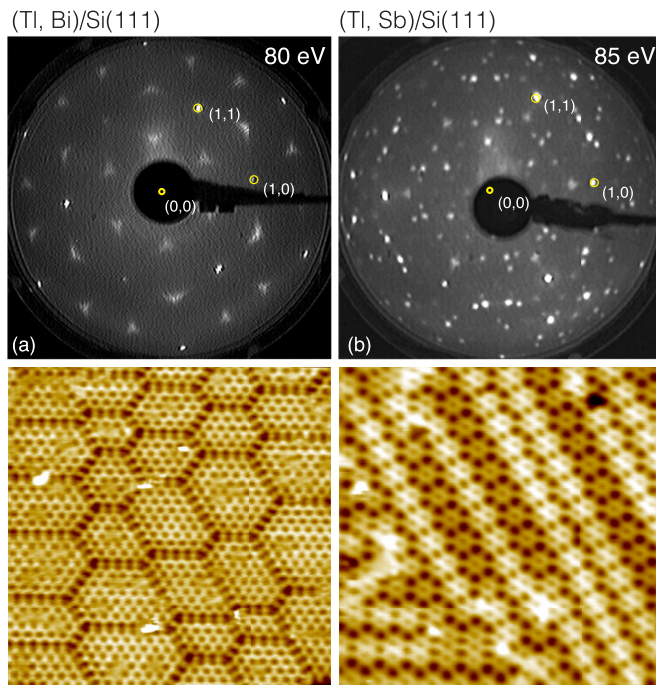


FIG. 6. LEED patterns and $200 \times 200 \text{ \AA}^2$ STM images from (a) $(\text{Ti, Bi})/\text{Si}(111)$ (empty states, $+0.8 \text{ V}$) and (b) $(\text{Ti, Sb})/\text{Si}(111)$ (filled states, -1.0 V) surfaces.

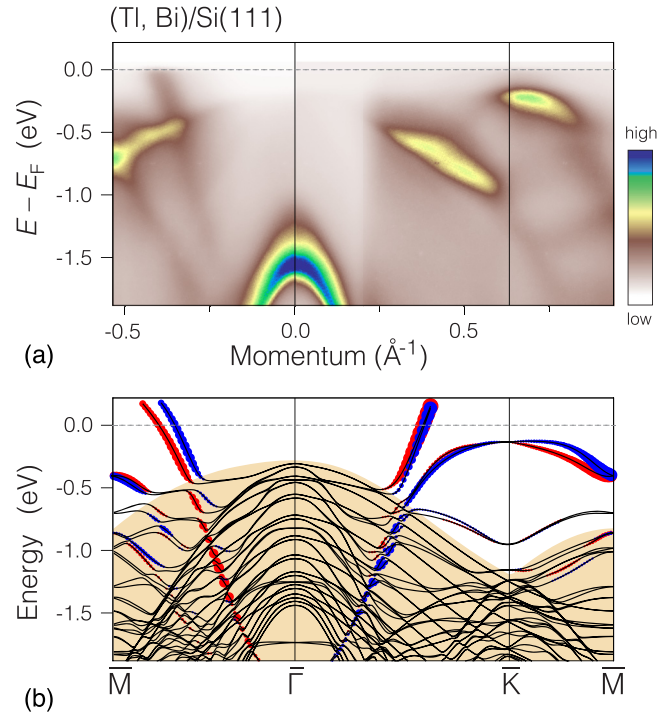


FIG. 7. (a) Experimentally determined and (b) calculated band dispersions for the $(\text{Ti, Bi})/\text{Si}(111)$ surface. The part of the ARPES spectrum recorded in the Γ - \bar{M} direction has been symmetrized with respect to \bar{M} point.

In STM images, these domains are seen as patches having honeycomb-like inner appearance [Fig. 6(a)]. Limited size of the structure domains leads to a specific triangular shape of LEED $1/3$ -order reflections as well as to smearing of the ARPES features. Nevertheless, the counterpart of the predicted spin-split metallic band is clearly seen in the experimental ARPES spectrum [17] (Fig. 7).

The $(\text{Ti, Sb})/\text{Si}(111)$ system can be expected to be akin the $(\text{Ti, Bi})/\text{Si}(111)$ one. Indeed, it also displays tiling-like structures, but the $\sqrt{3} \times \sqrt{3}$ -periodic structures in the $(\text{Ti, Sb})/\text{Si}(111)$ system are lacking. As an example, Fig. 6(b) shows an STM image and LEED pattern from a surface prepared by RT adsorption of $\sim 0.3 \text{ ML}$ of Sb onto $\text{Ti}/\text{Si}(111)1 \times 1$ followed by a brief annealing at $150 \text{ }^\circ\text{C}$. One can see that, though the surface has a composition suitable for the formation of the structure as in Fig. 1(a), it exhibits a complicated structure without any indication of the occurrence of the $\sqrt{3} \times \sqrt{3}$ domains. This behavior can be understood on the basis of the DFT calculations, which show that the tiling element containing Sb trimers is energetically favorable over the tiling element with Sb adatom by 21 meV per 1×1 unit cell. As a result, Ti-Sb compound with $1/3 \text{ ML}$ of Sb (i.e., built solely of the tiling element with a single Sb atom) does not form. However, the surface cannot also be built continuously of only the tiling elements with Sb trimers, hence the Ti-Sb surface structure incorporates a mixture of tiling elements.

The $(\text{Ti, Te})/\text{Si}(111)$ and $(\text{Ti, Se})/\text{Si}(111)$ systems have been found to demonstrate a very similar behavior with respect to each other. In the experiments with Te or Se dosing of $\text{Ti}/\text{Si}(111)1 \times 1$ surface held at temperatures ranging from RT

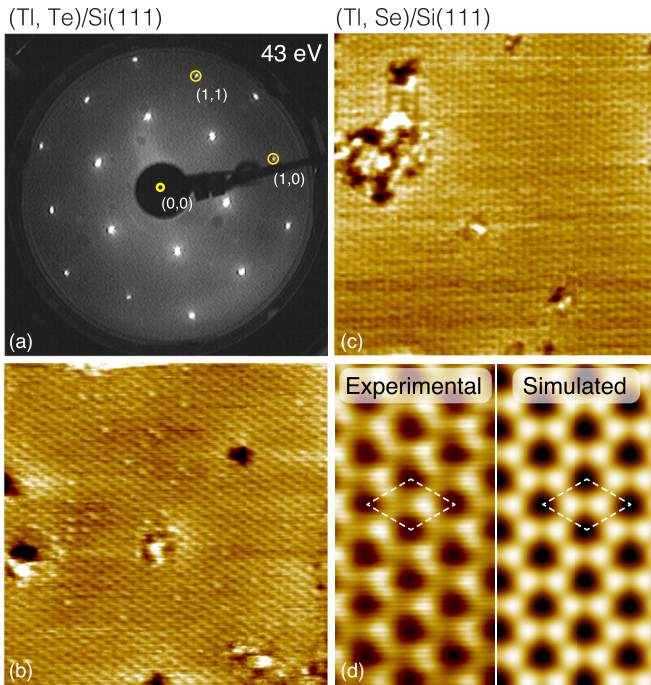


FIG. 8. (a) LEED pattern and (b) $250 \times 250 \text{ \AA}^2$ empty-state (-1.0 V) STM image from the (Tl, Te)/Si(111) surface. (c) $250 \times 250 \text{ \AA}^2$ empty-state (-0.8 V) STM image and (d) high-resolution STM image combined with a simulated STM image for a (Tl, Se)/Si(111) surface. The $\sqrt{3} \times \sqrt{3}$ unit cell is outlined by a dashed white frame.

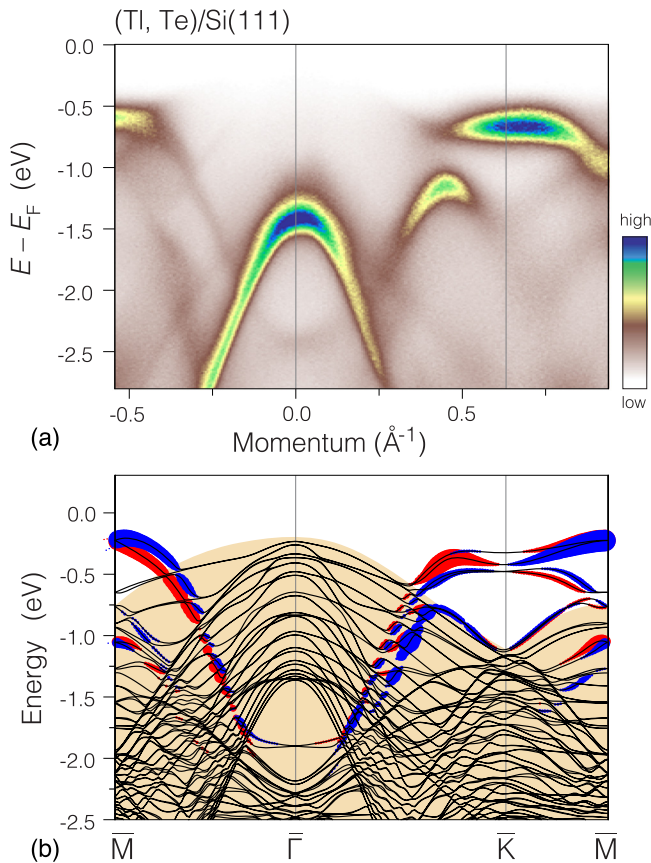


FIG. 9. (a) Experimentally determined and (b) calculated band dispersions for the (Tl, Te)/Si(111) surface.

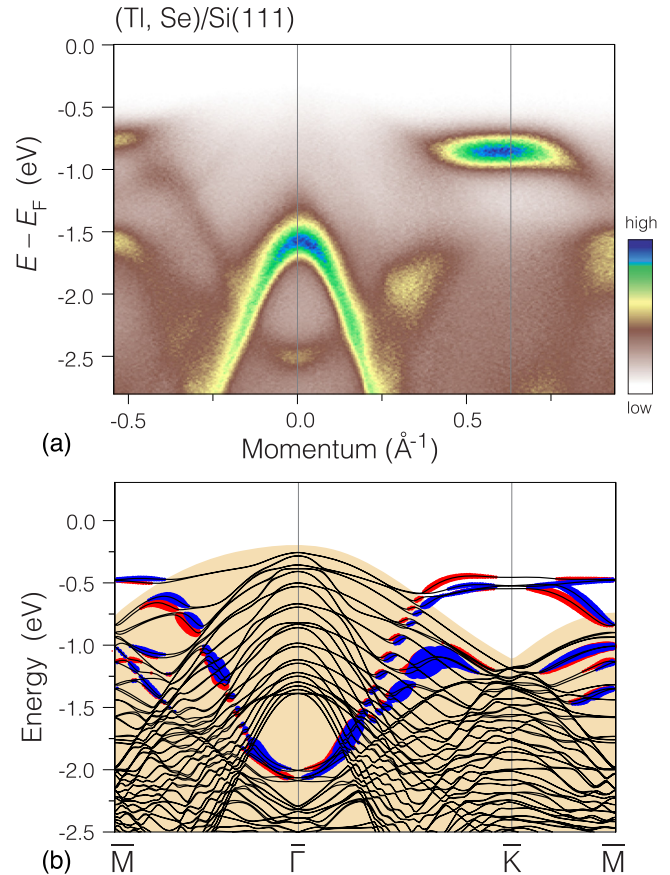


FIG. 10. (a) Experimentally determined and (b) calculated band dispersions for the (Tl, Se)/Si(111) surface.

to $\sim 150 \text{ }^\circ\text{C}$, the optimal dose when the RHEED 1/3-order reflections reach the maximum has been estimated with XPS to correspond to $\sim 1/3 \text{ ML}$ of Te or Se. In STM images (Fig. 8), the Tl-Te and Tl-Se compounds display a honeycomb-like appearance, in reasonable agreement with simulated STM images [see Fig. 8(d)]. However, one can notice a certain asymmetry in the experimental STM image, which is believed to be an artifact of recording and/or processing of the STM image from a surface with relatively low atomic corrugation.

Figures 9 and 10 present experimental ARPES spectra from (Tl, Te)/Si(111) and (Tl, Se)/Si(111) surfaces, respectively, in comparison with the corresponding calculated band structures. One can clearly see that there is proper consistency between experimental data and calculations in that the both surfaces are insulators. Moreover, a close coincidence between calculations and experiment even in fine features can be treated as a solid argument for the validity of the chosen structural model.

IV. CONCLUSIONS

In conclusion, we have tested if the 2D Tl- X compounds on Si(111), where $X = \text{Pb, Sn, Bi, Sb, Te, and Se}$, can have atomic arrangement similar to that of the (Tl, Pb)/Si(111) system, namely a $\sqrt{3} \times \sqrt{3}$ -periodic honeycomb network of chained Tl trimers with X atoms occupying the centers of the honeycomb units. Thus, the structure adopts 1.0 ML of Tl and $1/3 \text{ ML}$ of X species. Among the species under consideration, Sn and

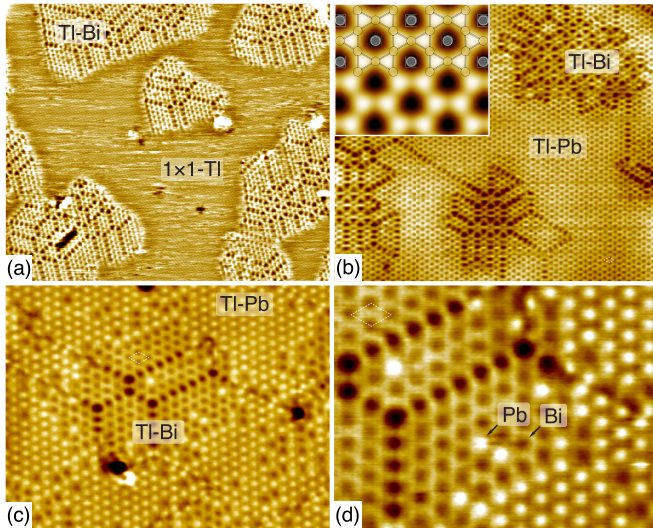


FIG. 11. (a) $380 \times 325 \text{ \AA}^2$ empty-state (+0.6 V) STM image from the Tl/Si(111) 1×1 surface after deposition of about 0.13 ML of Bi onto it. (b) $380 \times 325 \text{ \AA}^2$ empty-state (+0.6 V), (c) $190 \times 145 \text{ \AA}^2$ filled-state (-1.4 V), and (d) $95 \times 70 \text{ \AA}^2$ filled-state (-1.4 V) STM image of a surface as in (a) after sequential deposition of about 0.20 ML of Pb onto it. The inset in (b) illustrates the registry of the Tl-associated STM protrusions in simulated STM image with respect to the (Tl, X)/Si(111) structural model. In the model, Tl atoms are shown by yellow circles, X atoms by gray circles, and Tl trimers are hatched by white color. The STM image in (d) is a close-up view of the central part of the image in (c).

Sb have been found to form 2D compounds of other structural types, while for the species Pb, Bi, Te, and Se the 2D compound of the above type do have clear counterparts in reality. Structural and electronic properties of the compounds have been characterized in detail using theoretical DFT calculations and experimental STM and ARPES observations. It has been found that though structurally all Tl-X compounds are very similar, variation of the X species affects greatly the compound electronic properties. The Tl-Pb compound is strongly metallic with two metallic surface-state bands; the Tl-Bi compound is also metallic but with a single metallic band; the Tl-Te and Tl-Se compounds are insulators. A characteristic feature of all the compounds is a significant spin-splitting of their

surface-state bands that makes them of interest for possible spintronics applications.

As a final remark, we would like to note an additional promising feature of the Tl-X compound family. Its structure is essentially a Tl-based honeycomb matrix where each honeycomb can be filled by any X atom, including Pb, Bi, Te, or Se, as illustrated in the inset in Fig. 11(b). This provides a principal possibility for various types of engineering within a 2D compound layer using sequential deposition or codeposition of various X species. For example, these might be formation of 2D heterostructures with ideal stacking of areas covered by different Tl-X compounds, doping of one Tl-X compound by small amounts of other X species, or formation of ternary Tl-X₁-X₂ compounds. As an example, Fig. 11 shows STM images from the surface obtained by sequential deposition of Bi and Pb onto Tl/Si(111) 1×1 . At the first step, upon deposition of about 0.13 ML of Bi the patches of the Tl-Bi compound were formed, thus occupying about 40% of the surface area, the other area being still occupied by pristine Tl/Si(111) 1×1 reconstruction [Fig. 11(a)]. At the next step, upon deposition of about 0.20 ML of Pb onto this surface, the residual Tl/Si(111) 1×1 area transformed into the Tl-Pb compound. The patches of Tl-Bi compound are clearly distinguished from the Tl-Pb area by a presence of dense domain walls in the former and their absence in the latter [see the empty-state STM image in Fig. 11(b)]. A close-up look reveals a certain X-species intermixing between Tl-Bi and Tl-Pb regions. This is especially apparent in the filled-state (-1.4 V) STM images, where Bi atoms are seen as depressions and Pb atoms as protrusions [Figs. 11(c) and 11(d)]. However, a detailed analysis of the surface structures of these types lies far beyond the scope of this report and it actually requires comprehensive studies, in particular over the extended list of Tl-X compounds under consideration, that show good promise to obtain interesting results.

ACKNOWLEDGMENTS

The work was supported by the Russian Science Foundation under Grant No. 14-12-00479. The part of the work devoted to the study of the (Tl, Bi)/Si(111) and (Tl, Sb)/Si(111) systems was supported by the Russian Foundation for Basic Research under Grant No. 17-02-00567.

- [1] J. R. Osiecki, H. M. Sohail, P. E. J. Eriksson, and R. I. G. Uhrberg, Experimental and Theoretical Evidence of a Highly Ordered Two-Dimensional Sn/Ag Alloy on Si(111), *Phys. Rev. Lett.* **109**, 057601 (2012).
- [2] M. Zhou, W. Ming, Z. Liu, Z. Wang, P. Li, and F. Liu, Epitaxial growth of large-gap quantum spin Hall insulator on semiconductor surface, *Proc. Natl. Acad. Sci. USA* **111**, 14378 (2014).
- [3] M. Zhou, W. Ming, Z. Liu, Z. Wang, Y. Yao, and F. Liu, Formation of quantum spin Hall state on Si surface and energy gap scaling with strength of spin orbit coupling, *Sci. Rep.* **4**, 7102 (2014).
- [4] F. C. Chuang, L. Z. Yao, Z. Q. Huang, Y. T. Liu, C. H. Hsu, T. Das, H. Lin, and A. Bansil, Prediction of large-gap two-dimensional topological insulators consisting of bilayers of Group III elements with Bi, *Nano Lett.* **14**, 2505 (2014).
- [5] B. Huang, K. H. Jin, H. L. Zhuang, L. Zhang, and F. Liu, Interface orbital engineering of large-gap topological states: Decorating gold on a Si(111) surface, *Phys. Rev. B* **93**, 115117 (2016).
- [6] F. C. Chuang, C. H. Hsu, H. L. Chou, C. P. Crisostomo, Z. Q. Huang, S. Y. Wu, C. C. Kuo, W. C. V. Yeh, H. Lin, and A. Bansil, Prediction of two-dimensional topological insulator by

- forming a surface alloy on Au/Si(111) substrate, *Phys. Rev. B* **93**, 035429 (2016).
- [7] D. V. Gruznev, L. V. Bondarenko, A. V. Matetskiy, A. Y. Tupchaya, A. A. Alekseev, C. R. Hsing, C. M. Wei, S. V. Eremeev, A. V. Zotov, and A. A. Saranin, Electronic band structure of a Tl/Sn atomic sandwich on Si(111), *Phys. Rev. B* **91**, 035421 (2015).
- [8] L. V. Bondarenko, D. V. Gruznev, A. A. Yakovlev, A. Y. Tupchaya, D. Usachov, O. Vilkov, A. Fedorov, D. V. Vyalikh, S. V. Eremeev, E. V. Chulkov, A. V. Zotov, and A. A. Saranin, Large spin splitting of metallic surface-state bands at adsorbate-modified gold/silicon surfaces, *Sci. Rep.* **3**, 1826 (2013).
- [9] D. V. Gruznev, L. V. Bondarenko, A. V. Matetskiy, A. A. Yakovlev, A. Y. Tupchaya, S. V. Eremeev, E. V. Chulkov, J. P. Chou, C. M. Wei, M. Y. Lai, Y. L. Wang, A. V. Zotov, and A. A. Saranin, A strategy to create spin-split metallic bands on silicon using a dense alloy layer, *Sci. Rep.* **4**, 4742 (2014).
- [10] D. V. Gruznev, L. V. Bondarenko, A. V. Matetskiy, A. Y. Tupchaya, E. N. Chukurov, C. R. Hsing, C. M. Wei, S. V. Eremeev, A. V. Zotov, and A. A. Saranin, Atomic structure and electronic properties of the two-dimensional (Au, Al)/Si(111) 2×2 compound, *Phys. Rev. B* **92**, 245407 (2015).
- [11] A. V. Matetskiy, S. Ichinokura, L. V. Bondarenko, A. Y. Tupchaya, D. V. Gruznev, A. V. Zotov, A. A. Saranin, R. Hobar, A. Takayama, and S. Hasegawa, Two-Dimensional Superconductor with a Giant Rashba Effect: One-Atom-Layer Tl-Pb Compound on Si(111), *Phys. Rev. Lett.* **115**, 147003 (2015).
- [12] G. Kresse and J. Furthmüller, Efficient iterative schemes for *ab initio* total-energy calculations using a plane-wave basis set, *Phys. Rev. B* **54**, 11169 (1996).
- [13] G. Kresse and D. Joubert, From ultrasoft pseudopotentials to the projector augmented-wave method, *Phys. Rev. B* **59**, 1758 (1999).
- [14] L. G. Ferreira, M. Marques, and L. K. Teles, Approximation to density functional theory for the calculation of band gaps of semiconductors, *Phys. Rev. B* **78**, 125116 (2008).
- [15] L. G. Ferreira, M. Marques, and L. K. Teles, Slater half-occupation technique revisited: The LDA-1/2 and GGA-1/2 approaches for atomic ionization energies and band gaps in semiconductors, *AIP Adv.* **1**, 032119 (2011).
- [16] S. Adachi, R. Blachnik, R. P. Devaty, F. Fuchs, A. Hangleiter, W. Kulisch, Y. Kumashiro, B. K. Meyer, and R. Sauer, in *Semiconductors: Intrinsic Properties of Group IV Elements and III-V, II-VI, and I-VII Compounds*, Landolt-Börnstein, New Series, Group III: Semiconductors, Subvolume A1, Part β (Springer, Berlin, 1999).
- [17] D. V. Gruznev, L. V. Bondarenko, A. V. Matetskiy, A. N. Mihalyuk, A. Y. Tupchaya, O. A. Utas, S. V. Eremeev, H. R. Hsing, J. P. Chou, C. M. Wei, A. V. Zotov, and A. A. Saranin, Synthesis of two-dimensional $\text{Tl}_x\text{Bi}_{1-x}$ compounds and Archimedean encoding of their atomic structure, *Sci. Rep.* **6**, 19446 (2016).